DISCHARGE OF A PLANE AIR JET INTO A BLIND PASS

E. P. Dyban, A. I. Mazur,
and É. Ya. Épik

UDC 533.601.1

The existence of two discharge regimes of a plane jet into a blind pass was established experimentally. It is shown that the initial section is absent in such a jet and the range of the jet is commensurable with its width.

The hydrodynamics of a plane jet emerging into a blind pass has been studied considerably less thoroughly than that of an axisymmetric jet. In particular, whereas for an axisymmetric jet emerging into a relatively long cylindrical blind pass there are experimental data in the literature (see, for example, [1, 2]) agreeing satisfactorily with the theoretical solution [2], the information on the propagation of a plane jet in a plane-parallel blind pass is limited to the solutions in [2-4].

An analysis of the results of the solutions in [2] and [3, 4] shows that they differ considerably. Thus, according to [2] the length of the initial section in the jet emerging into a long blind pass remains approximately the same as in a free jet, and complete attenuation of the axial velocity occurs at a distance of 3-4 diameters of the blind pass. It follows from the solutions in [3, 4] obtained for blind passes of arbitrary length that the initial section is practically absent in the jet, and the drop of axial velocity occurs so intensely that already at distances of the order of one diameter of the blind pass from the nozzle end face it is 1-3% of the initial discharge velocity. In particular, for a plane jet discharging into a plane-parallel blind pass [4] the change of axial velocity over the length of the blind pass is described by the expression

$$\bar{u}_m = \sum_{n=1}^{\infty} \frac{2\sin(\pi n\bar{b})\,\mathrm{sh}\left[\pi n(\bar{h}-\bar{x})\right]}{\pi n(1-\bar{b})\,\mathrm{sh}(\pi n\bar{h})}. \quad (1)$$

Having assigned in the first approximation a rectangular velocity diagram in the cross section of the blind pass coinciding with the nozzle end face, we obtain, for example, when $\bar{b} = 0.3$

$$\bar{u}_m \simeq 0.91 \sum_{n=1}^{\infty} \frac{\sin(\pi n\bar{b})}{n\exp(\pi n\bar{x})}. \quad (2)$$

Since the solution in [2] is inapplicable for relatively short blind passes and there is a fundamental difference between the results of the solutions in [2] and [4], the need for an experimental investigation of the hydrodynamics of a plane jet discharging into a blind pass of arbitrary length is obvious.

In the present study this investigation was performed on plane-parallel rectangular blind passes with a length of 191 mm and width of 25 and 51 mm and on a parabolic-type blind pass with a diameter of a circle inscribed at the vertex of 24 mm and width of 86 mm at a maximum length of 191 mm; the height of the blind passes was 60 mm. The slotted nozzle, installed in the plane of symmetry of the blind pass, had movable sides, which made it possible to change the width of the nozzle from 5 to 25 mm; the distance from the nozzle end face to the critical point (vertex of the blind pass) in the parabolic blind pass was changed by means of inserts; in the rectangular blind pass the end wall could be moved, creating blind passes of arbitrary length up to the maximum. The surface of the blind passes about the perimeter was drained by 0.6-mm-diam. holes. The pipe connections for bleeding the static pressure were connected to a 40-point multitube pressure gauge which recorded the distribution of the static pressure over the perimeter of the blind pass.

Institute of Technical Thermal Physics, Academy of Sciences of the Ukrainian SSR, Kiev. Translated from Inzhenerno-Fizicheskii Zhurnal, Vol. 20, No. 6, pp. 1020-1026, June, 1971. Original article submitted July 31, 1970.

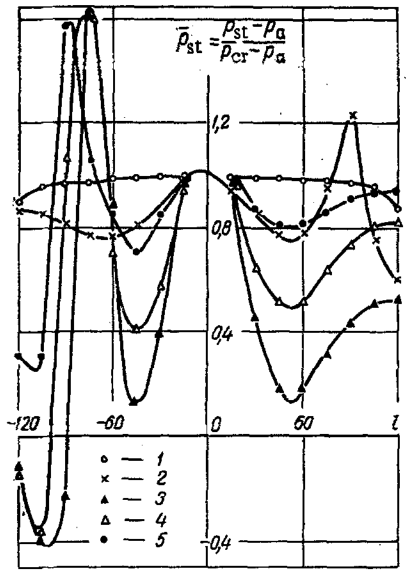

Fig. 1. Typical distribution of static pressure over the perimeter of the blind pass, mm (h = 112 mm): 1) symmetric discharge with counterpressure, $\bar{b}$ = 0.31; 2) discharge with attachment of the jet into a parabolic blind end with increased counterpressure, $\bar{b}$ = 0.12; 3) the same, into a rectangular blind pass without counterpressure, $\bar{b}$ = 0.14; 4) the same, with counterpressure, $\bar{b}$ = 0.14; 5) the same, with increased counterpressure, $\bar{b}$ = 0.14.

The axial velocity and its fluctuation over the length of the blind pass were measured by a constant-temperature hot-wire anemometer whose sensor (wire diameter 6 μm, length 2-2.5 mm) was moved by a coordinator fastened on the end wall of the blind pass. The hot-wire anemometer measurements were duplicated in control experiments by a straight combined Prandtl tube with a 0.6 mm diameter of the central opening. The possibility of measuring the velocity profile in the exit channels of the blind pass was also provided for in the device.

The air was bled from the blind passes through side channels with 45-mm-diam. discharge holes, which during the experiments were either open (regimes without counterpressure) or drain tubes with adjustable valves were connected to them (regimes with counterpressure).

The initial discharge velocity from the nozzle did not exceed 100 m/sec, the air temperature was 15-20°C; this corresponded to Reynolds numbers, determined from the parameters of the nozzle discharge, of $3 \cdot 10^{-3}$-10^5; the initial turbulence varied from 2 to 13% with a change of nozzle width from 6 to 23 mm, respectively.

For visual observations of the character of propagation of the jet in the blind pass, in one of its side walls we cut a 1.5-mm-wide slot over the entire length of the blind pass, which was sealed tight on the outside by a strip of organic glass. In these experiments water with the addition of purified aluminum powder was passed through the blind pass. The flow was illuminated through the slot by a 2 kW incandescent lamp and photographed by a "Zenith-ZM" camera on ORWO film with a sensitivity of 360 units according to the State Standard.

The experiments showed that with the discharge of a plane jet into a blind pass two flow regimes are observed which were not predicted by a single one of the solutions in [2, 3, 4].

We see from the curves of the distribution of the static pressure over the perimeter of the blind pass presented in Fig. 1 that the first regime, henceforth called symmetric discharge, is characterized by a pressure distribution completely symmetric relative to the critical point (curve 1). The second regime, henceforth called discharge with attachment of the jet (curves 2-5), is characterized by the presence on one of the side walls of a noticeable pressure peak whose position relative to the longitudinal axis of the blind pass (to the right or left) is equiprobable and well-defined relative to the nozzle end face.

The relative width of the nozzle $\bar{b}$ is the parameter determining the occurrence of one of the indicated discharge regimes. In all investigated cases a symmetric discharge was observed when $\bar{b} > 0.3$ and a discharge with attachment of the jet when $\bar{b} < 0.27$.

The transfer of the pressure peak from one side wall of the blind pass to the other at a point symmetric to the original is possible in regimes with attachment of the jet. This transfer can be effected in particular by a slight increase of counterpressure in the exit channel on that side wall of the blind pass where the pressure peak is located. In this case the curve of the distribution of the static pressure over

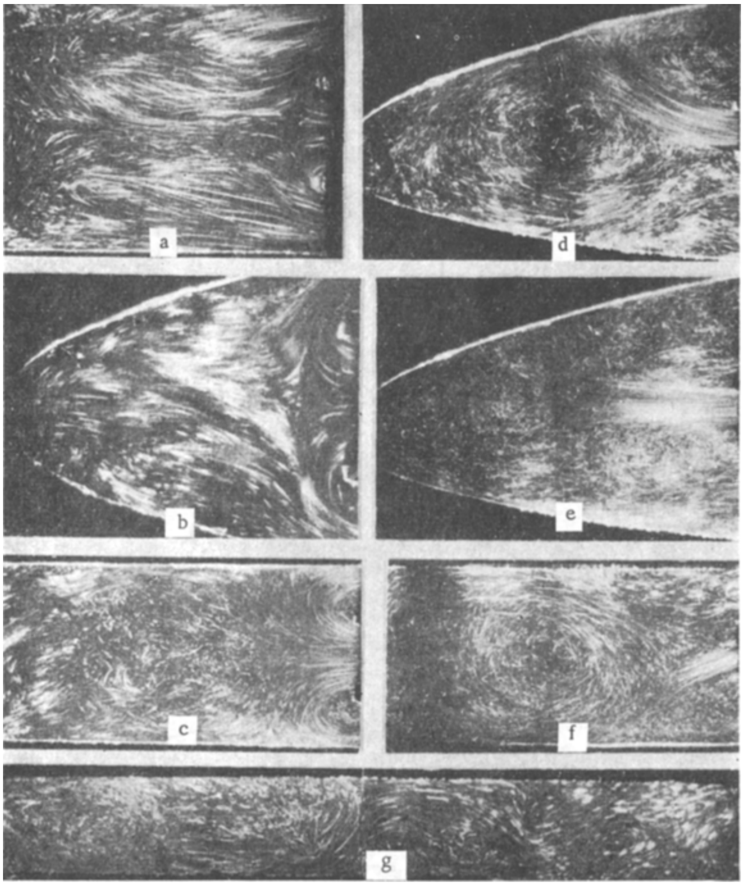

Fig. 2. Discharge of a plane jet into a blind pass, Re = (4.1-5) $\cdot 10^3$: a) h = 64 mm; b = 17.5 mm; B = 51 mm; b) respectively 63; 23; 61 mm; c) 112; 18; 51 mm; d) 112; 23.5; 76 mm; e) 112; 11; 76 mm; f) 112; 7; 51 mm; g) 191; 5.5; 25 mm.

the perimeter of the blind pass becomes a mirror image of the curve preceding it – the pressure peak moves to the opposite wall of the blind pass, and the process itself is accompanied by an acoustic effect, a small bang. An increase of the velocity at the nozzle exit causes an increase of the absolute value of the pressure peak without changing its location and length. During operation of the device with counterpressure the flow in the blind pass and the transfer effect of the pressure peak are sufficiently stable in time. During operation of the device with direct exhaust into the atmosphere spontaneous transfer of the pressure peak from one side to the other is observed: regular in a relatively long blind pass and systematic in a short one, with a length of 1.1-1.3 diameters of the blind pass.

Figure 2 (a, b, c) shows typical photographs of the symmetric regime of discharge of the jet into a blind pass, where we see the absence of the initial section in the jet. The range of the jet is commensurable with the width of the nozzle, and a turn of the flow occurs in the immediate vicinity of the nozzle end face. A large part of the blind pass is occupied by a system of eddies having a relatively low velocity; the boundary of existence of the jet and start of the eddy zone is defined quite distinctly. Symmetry of the turn of the jet provides also equality of the flow rates in the exit channels of the blind pass.

Photographs of discharge with attachment of the jet are presented in Fig. 2 (d, f, g). In this case the jet emerging into the blind pass curves immediately at the nozzle exit and attaches to one of the side walls of the blind pass. Its further path represents a characteristic looplike curve enveloping either the entire cavity of the blind pass or the region near the nozzle. Visual observations show that the phenomenon of attachment of a narrow plane jet to one of the side walls of a blind pass is analogous to the Coanda effect and apparently has the same nature of occurrence [5].

The investigations established that in blind passes when $\overline{h} > 1.5$ and $\overline{b} = 0.07$–0.27 there is no symmetric regime of discharge of a plane jet analogous to that shown in Fig. 2e, where the moment of transfer of the jet from one side wall of the blind pass to the other is recorded.

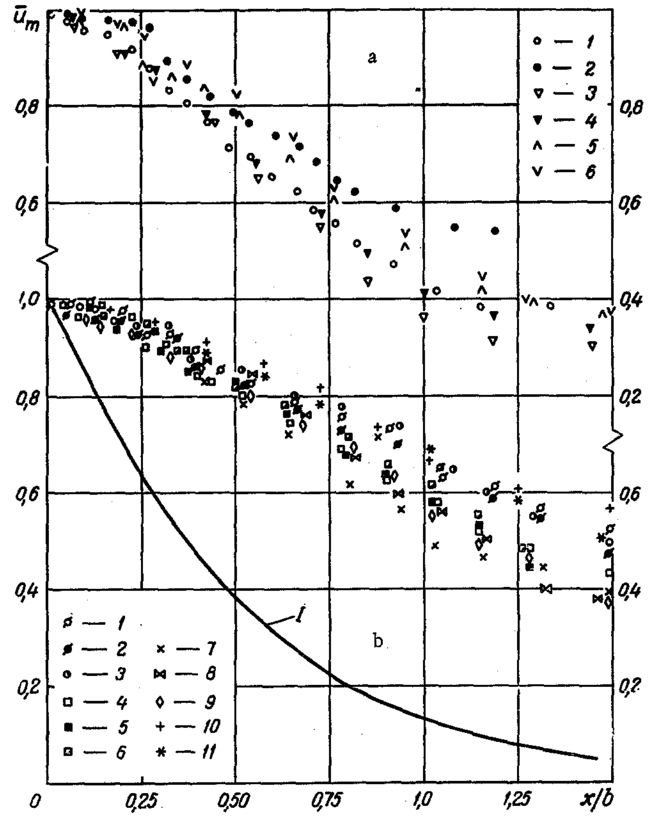

Fig. 3. Change of the axial velocity over the length of the blind pass with a symmetric regime of jet discharge: I) according to Eq. (2) for $\bar{b} = 0.3$; a) parabolic blind pass: 1, 2) h = 63 mm; B = 61 mm; b = 18.5 mm; u_0 = 22 and 41 m/sec; 3, 4) respectively 112; 76; 21 mm; u_0 = 23 and 36 m/sec; 5, 6) 162; 85; 23.3 mm; u_0 = 24.2 and 40.2 m/sec; b) rectangular blind pass: 1, 2, 3) h = 64 mm; u_0 = 18.1; 34.7; 57.3 m/sec; 4, 5, 6) 112; u_0 = 16.7; 33.9; 55.7 m/sec; 7, 8, 9) 191; u_0 = 24.8; 40.3; 60.2 m/sec; 1-9) for b = 15.2 mm; B = 51 mm; 10, 11) h = 191 mm; B = 25 mm; b = 6.9 mm; u_0 = 15.4 and 28 m/sec.

An analysis of the photographs of the discharge of the jet with attachment shows that the pressure peak in the curves of Fig. 1 is due to attachment of the jet to the side wall of the blind pass. In addition, it is explained why the transfer of the jet occurs only under an effect on the exit channel located on the side of attachment of the jet: an increase of counterpressure in this channel squeezes (removes) the point of attachment of the jet closer to the end wall of the blind pass, straightening the jet. Passing through the unstable zone on the axis of symmetry of the blind pass (Fig. 2e), the jet attaches stably to the other side wall.

In the experiments on discharge of a jet with attachment we observed extremely marked asymmetry of the flow rates in the exit channels of the blind pass: in the case of operation of the device with counterpressure the flow rates differed by a factor of 1.7-1.8 and without counterpressure by a factor of 4, whereby greater flow rates occurred in the exit channel adjacent to the side wall free of attachment.

Figure 3 shows the results of measuring the velocity on the axis of the jet discharging into a blind pass for the symmetric regime.* Without analyzing the slight (very weak) effect of the Reynolds number, initial turbulence, geometric relations, and shape of the blind passes on the character of change of the axial velocity, we should note the trend toward a marked drop of velocity over the length of the jet which was common

*Measurements of the velocity were limited to the length of existence of the jet. The boundary between the jet and eddy zone was determined by comparing the readings of the combined tube with the data of the hot-wire anemometer measurements.

for all experiments: in the range $\bar{h}$ = 1.5-7.6 for x/b = 1.5 $\bar{u}_m$, $u_m \simeq$ 0.3-0.5. In this case the character of change of the velocity along the axis of the jet agrees qualitatively better with the results of the solutions in [3, 4] than of the solution in [2]. As is known, it is suggested in [3, 4] that the motion of a fluid is described by equations of the potential flow directly from the nozzle end face; in [2] such an assumption is made only for the section of the turn of the jet in the blind pass, i.e., at a distance of more than two diameters of the blind pass from the nozzle end face.

We note that the existence of two discharge regimes and the absence of an initial section in the jet were observed also in a blind pass for which at a height of 60 mm and B = 16 mm the nozzle width was varied from 2 to 6 mm.

The data presented above on the regularities of the discharge of a plane jet into a blind pass permits explaining the U-shaped curves of the distribution of local heat-transfer coefficients about the perimeter of a parabolic blind pass observed in [6]. It turns out that in the experiments in [6], which were carried out under conditions of a symmetric jet-discharge regime, the maximum values of the local heat-transfer coefficient were due to contact of the jet after the turn with the side walls of the blind pass to the right and left of the nozzle.

On the basis of the experimental data obtained we can make the following conclusions.

1. In the case of the propagation of a plane jet into a plane-parallel blind pass of the investigated dimensions and configurations there exist two discharge regimes – symmetric and with unilateral attachment of the jet; the boundary value of the characteristic parameter is $\bar{b} \simeq$ 0.27-0.3.

2. In the case of a symmetric discharge regime into a blind pass with a relative length $\bar{h}$ = 1.5-7.6 the initial section is absent in the plane jet, and the range of the jet does not exceed 1.0-1.5 of the nozzle width.

3. The shape of the blind pass, its length, initial flow turbulence, Reynolds number, and counterpressure at the exit of the blind pass do not have a substantial effect on the character of the flow in it in the investigated range of values: $\bar{h}$ = 1.5-7.6; $\bar{b}$ = 0.07-0.5; Re = $3 \cdot 10^3$-10^5.

NOTATION

h	is the length of blind pass;
B	is the width of blind pass;
b	is the width of plane nozzle;
x	is the current length of blind pass reckoned from the nozzle end face;
$\bar{h}$, $\bar{x}$	are the lengths of blind pass referred to its width;
u_m	is the axial velocity;
u_0	is the initial discharge velocity of jet (at nozzle end face);
$\bar{u}_m$	is the axial velocity referred to the initial discharge velocity of the jet;
δ	is the thickness of nozzle edge at end face;
$\bar{b} = (b/B-2\delta)$	is the width of nozzle referred to the effective width of the exit channels in the nozzle end face section;
p_{st}	is the static pressure on the wall of the blind pass;
p_{cr}	is the pressure at the critical point;
p_a	is the atmospheric pressure;
R_e	is the Reynolds number calculated on the basis of the discharge velocity and hydraulic diameter of the plane nozzle;
l	is the current length along perimeter of blind pass reckoned from the critical point.

LITERATURE CITED

1. V. A. Bakharev and V. N. Troyanovskii, Principles of the Design and Calculation of Heating and Ventilation with a Concentration Air Exhaust [in Russian], Profizdat (1958).
2. G. N. Abramovich, Theory of Turbulent Jets [in Russian], Fizmatgiz, Moscow (1960).
3. V. A. Chernykh, Izv. Akad. Nauk SSSR, Mekhan. Zhidk. i Gaza, No. 2 (1966).
4. A. I. Mazur, in: Problems of Technical Thermal Physics [in Russian], No. 2, Naukova Dumka (1969).
5. K. K. Shal'nev et al., Dokl. Akad. Nauk SSSR, 175, No. 1 (1967).
6. E. P. Dyban and A. I. Mazur, Inzh.-Fiz. Zh., 17, No. 5 (1969).